Open Journal of Civil Engineering, 2026, 16(3), 454-473
https://www.scirp.org/journal/ojce
ISSN Online: 2164-3172
ISSN Print: 2164-3164

Assessment of Groundwater Quality and the Influence of Land-Use Types on the Nairobi Aquifer, Kenya, Using GIS-Based Index Techniques

Mungathia Dickson Mugambi, Kipkulei Jeremiah Kiptala, Messo James Raude

Department of Civil, Construction and Environmental Engineering, Jomo Kenyatta University of Agriculture and Technology, Nairobi, Kenya
Email: dmugambi2526@gmail.com

How to cite this paper: Mugambi, M.D., Kiptala, K.J. and Raude, M.J. (2026) Assessment of Groundwater Quality and the Influence of Land-Use Types on the Nairobi Aquifer, Kenya, Using GIS-Based Index Techniques. *Open Journal of Civil Engineering*, **16**, 454-473.
https://doi.org/10.4236/ojce.2026.163024

Received: June 27, 2026
Accepted: August 1, 2026
Published: August 4, 2026

Copyright © 2026 by author(s) and Scientific Research Publishing Inc.
This work is licensed under the Creative Commons Attribution International License (CC BY 4.0).
http://creativecommons.org/licenses/by/4.0/
Open Access

Abstract

The Nairobi Aquifer is a strategic source of water for a metropolitan population exceeding four million, yet its sustainability is increasingly threatened by rapid urbanisation and intensifying land-use change. This study quantifies groundwater quality and evaluates the influence of land-use type on that quality using a Geographic Information System (GIS)-based Groundwater Quality Index (GQI). Six physico-chemical parameters: pH, electrical conductivity (EC), chloride, fluoride, nitrate and manganese, were obtained from borehole completion reports for seventeen boreholes distributed across Nairobi County and benchmarked against World Health Organization (WHO, 2017) drinking-water guidelines. A weighted-arithmetic index was computed for each borehole and interpolated across the aquifer using inverse-distance weighting (IDW). Land-use classes were derived from a 2020 land-cover map and overlaid on the GQI surface using zonal statistics. The computed GQI ranged from 13 to 492, indicating pronounced spatial heterogeneity. Built-up land exhibited the poorest mean groundwater quality (mean GQI = 150.2), classified as "unsuitable", whereas forest cover yielded the best quality (mean GQI = 38, "good"); open space and agriculture returned intermediate values of 61.3 and 52, respectively. Elevated indices coincided with densely settled, high-imperviousness districts where contamination is attributable to on-site sanitation, solid-waste leachate and surface runoff, while the large within-class variance of built-up land (standard deviation = 132.6) reflects the heterogeneity of urban contaminant sources. The results provide a spatially explicit, decision-ready basis for prioritising groundwater protection and integrating aquifer safeguards into urban land-use planning.

Keywords

Groundwater Quality Index, Land-Use Change, Nairobi Aquifer, GIS, Inverse-Distance Weighting, Urbanisation, Water Resources Management

1. Introduction

Groundwater accounts for the overwhelming majority of the planet's accessible freshwater and underpins both human livelihoods and economic activity, particularly where surface-water resources are scarce or unreliable [1]. Global demand for groundwater has risen steadily over the past five decades and is expected to continue increasing under the combined pressures of population growth, urban expansion and a higher frequency of drought [1]. The appeal of the resource lies in its generally high natural quality, its resilience during dry periods, and the comparatively low capital cost of its abstraction and development [2] [3].

In Africa, groundwater is the principal source of drinking water and its use for irrigation is projected to expand markedly as the continent confronts food insecurity [4]. Nevertheless, an estimated 300 million Africans still lack access to safe and reliable drinking water, and securing additional supplies is widely recognised as central to alleviating water scarcity [4] [5]. Kenya is classified as a water-scarce country; approximately 17 million people in its arid and semi-arid lands depend on groundwater as their primary source, while around 43% of rural and 24% of urban households rely on springs, wells or boreholes [6]. Beyond domestic supply, groundwater in Kenya sustains commercial horticulture, garden irrigation, and the water needs of residential estates and hotels in urban centres [1].

The Nairobi Aquifer system is a strategic resource for a metropolitan population that now exceeds four million. Its long-term sustainability, however, is challenged by rapid urban growth, escalating demand and contamination risks linked to anthropogenic activity. Like surface-water systems, aquifers are vulnerable to pollution from agricultural return flows, industrial effluents and inadequate waste management; once contaminated, groundwater is costly, technically demanding and slow to remediate, frequently requiring technologies that are not readily available in developing settings [7]. The consequences of such pollution: degraded water quality, public-health hazards and elevated treatment costs, can translate into artificial water scarcity, economic loss and ecological damage [8].

Protecting groundwater therefore depends on preventing and mitigating surface-derived contamination before it reaches the saturated zone. A practical first step is the spatially explicit characterisation of groundwater quality and of the pressures that drive its degradation. Index-based approaches have become a standard tool for this purpose because they condense multiple, dimensionally heterogeneous quality determinands into a single, interpretable measure. The Water Quality Index (WQI), introduced by Horton and formalised through the weighted-arithmetic formulation of Brown *et al.* [9], remains widely used; when implemented within a Geographic Information System (GIS) and combined with spatial interpolation, it yields a continuous Groundwater Quality Index (GQI) surface that supports mapping, comparison and management [10] [11].

Land use exerts a first-order control on groundwater quality, and the intensity of its influence varies systematically with land-cover type. Conversion to impervious, densely settled or intensively cultivated land alters both recharge and the loading of contaminants to the subsurface [12]. Although a borehole samples groundwater at a single point, the quality measured there integrates processes operating across its contributing area, so that the surrounding land use and catchment context, especially in low-relief terrain, are decisive [12]. Coupling a GIS-based GQI with a land-use classification through map overlay and zonal statistics provides a transparent means of attributing groundwater-quality variation to specific land-use categories, and of identifying where protective intervention is most urgent [13] [14].

Against this background, the present study pursues two objectives for the Nairobi Aquifer: 1) to determine the groundwater quality index of the aquifer using GIS techniques; and 2) to evaluate the influence of different land-use types on groundwater quality. Six physico-chemical parameters: pH, electrical conductivity, chloride, fluoride, nitrate and manganese, are assessed for seventeen boreholes, benchmarked against WHO drinking-water guidelines, integrated into a weighted-arithmetic GQI, interpolated across the aquifer, and overlaid on a contemporary land-use classification. The resulting maps and statistics are intended to furnish a decision-ready evidence base for integrating groundwater protection into urban land-use planning in a rapidly growing African city.

2. Study Area

Nairobi City, the capital of Kenya, lies in the south-central part of the country in East Africa and covers approximately 703.9 km^2. It is situated about 480 km northwest of Mombasa, between longitudes 36˚41'35"E and 37˚04'34"E and latitudes 01˚19'35"S and 01˚14'41"S. According to the 2019 Kenya Population and Housing Census, the city is home to about 4.397 million residents. The location of the study area is shown in **Figure 1**.

Geological and Hydrogeological Setting

The Nairobi Aquifer is governed by a complex assemblage of volcanic and sedimentary formations within the Nairobi Basin, which collectively determine its hydrodynamics and water chemistry. The principal water-bearing units are volcanic rocks—chiefly trachytes and basalts—formed during successive episodes of volcanic activity. These materials are characterised by relatively high porosity and permeability that favour groundwater storage and transmission. Interbedded sedimentary deposits, dominated by clays, siltstones and sandstones, interact with the volcanic sequence and impart marked variability in hydraulic conductivity across the system.

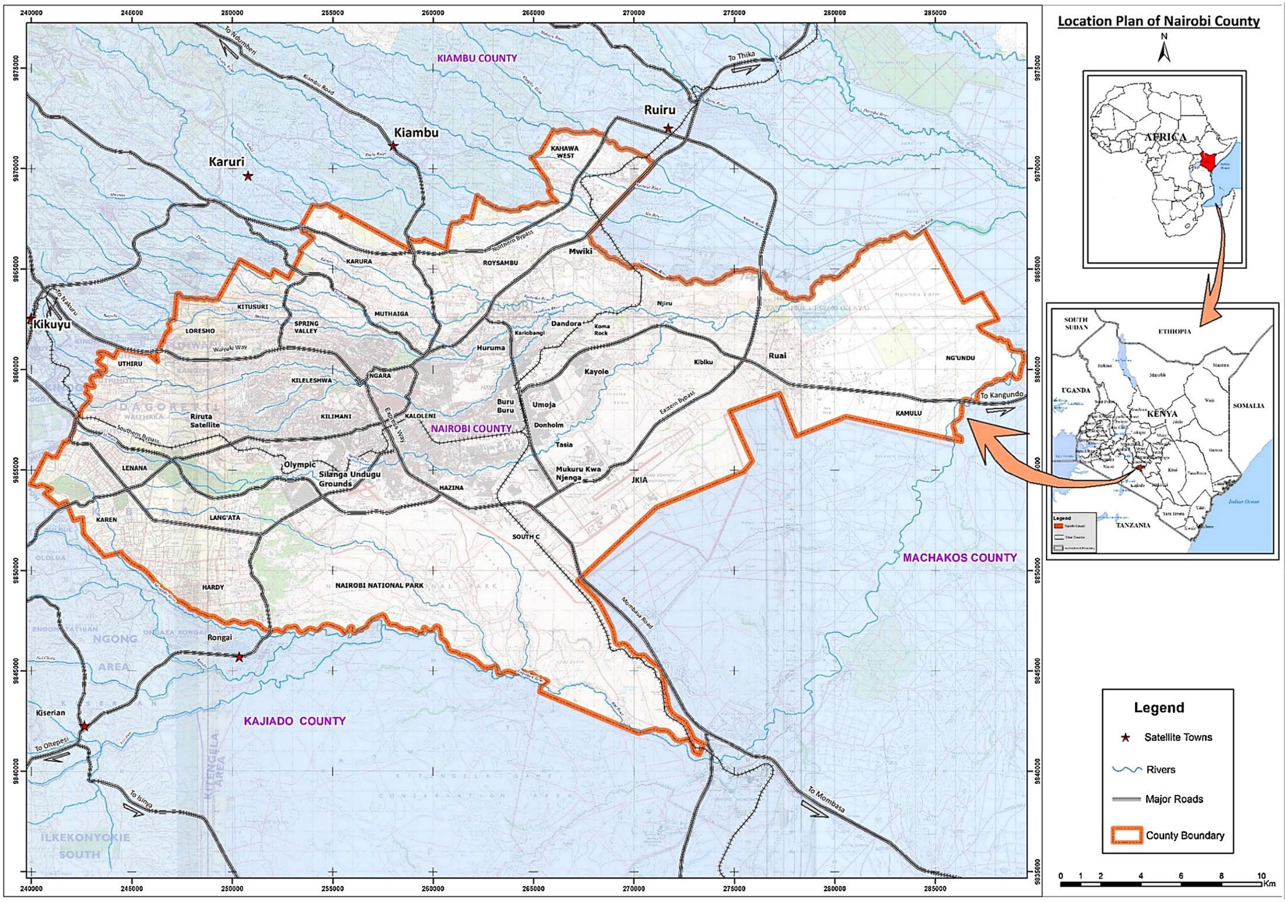

Figure 1. Location map of the study area, Nairobi County, Kenya.

Structural features such as faults and fractures further enhance transmissivity by establishing preferential flow paths; while these accelerate groundwater movement, they may also facilitate the rapid migration of contaminants. Hydrogeologically, the aquifer behaves as a multi-layered system in which weathered volcanic materials in the upper part provide the principal storage, underlain by deeper, less permeable strata that modulate both the quantity and quality of the resource. The interaction between these layers controls recharge and overall aquifer sustainability.

Recharge occurs primarily through direct infiltration of precipitation and surface runoff, especially in areas with limited urban development; it is strongly seasonal, peaking during the wet seasons. Progressive urbanisation has increased the proportion of impervious surface, which suppresses natural recharge and modifies the pathways by which contaminants reach the water table. The depth to the water table varies spatially in response to lithology and land use: zones of higher permeability tend to exhibit shallower water tables and more vigorous flow, whereas clay-rich domains are associated with deeper levels and slower movement. Because water–rock interaction governs the concentration of dissolved constituents, including nitrate and trace metals, districts subject to intensive urban or agricultural activity are particularly prone to quality deterioration—underscoring the need for continuous monitoring and proactive management.

3. Materials and Methods

3.1. Data Acquisition and Preparation

The datasets used to meet the study objectives were assembled in raster, vector and tabular formats from the sources summarised in Table 1. Borehole water-quality records were extracted from completion reports held by the Water Resources Authority (WRA), and borehole positions were verified in the field with a handheld Global Positioning System (GPS) receiver. Ancillary geospatial layers—digital terrain, soils, rainfall and land cover—were obtained from established national and international repositories to support spatial analysis and contextual interpretation.

Table 1. Datasets and sources used in the study.

Dataset	Source
Digital terrain model (DTM)	USGS SRTM DEM (a product of METI and NASA); earthexplorer.usgs.gov
Soil data	Digital Soil Map of the World (FAO-UNESCO, 1:5,000,000)
Rainfall data	TRMM precipitation product (NASA)
Land-use/land-cover map	Land-cover map of Nairobi (2020), Real Plan Consultants Ltd.
Landsat 8 imagery	earthexplorer.usgs.gov; RCMRD
Borehole data	WRA completion reports and GPS field survey
High-resolution imagery and topographic sheets	earthexplorer.usgs.gov; RCMRD; Google Earth

3.2. Determination of Groundwater Quality Index

Seventeen boreholes were selected from the WRA database to characterise the state of the groundwater. For each borehole, six determinands reported in the completion records were retained for analysis: pH, electrical conductivity (EC), chloride (Cl^-), fluoride (F^-), nitrate (NO_3^-) and manganese (Mn). These were chosen because they jointly capture the salinity, nutrient and trace-metal dimensions of drinking-water quality and are consistently reported across the network. Measured values were compared with the World Health Organization (WHO, 2017) drinking-water guidelines.

The six determinands were dictated by the contents of the completion-report archive, which does not record several constituents important for a complete potability assessment notably temperature, turbidity, microbiological indicators such as Escherichia coli, and dissolved heavy metals. Their omission is a direct consequence of reliance on secondary data and is discussed as a limitation in Section 4.4.

The seventeen boreholes do not derive from a formal, power-based sampling design; they represent the subset of the WRA completion-report archive that satisfied three practical criteria: 1) a complete record for all six target determinands; 2) a georeferenced position that could be verified in the field with GPS; and 3) a combined spatial distribution spanning the principal land-use zones of the county. This purposive, data-availability-driven selection maximises use of the available archive but does not guarantee statistical representativeness of the multi-layered aquifer, and the network remains sparse relative to the ≈704 km^2 study area. Basic borehole metadata; drilling and completion dates, total depth and screened interval, are only partially reported in the source documents; this incompleteness limits assessment of whether the seventeen sites sample comparable hydrostratigraphic horizons and is treated explicitly as a limitation (Section 4.4). Because the completion reports were issued in different years, the chemical records are not all contemporaneous with the 2020 land-cover map used in the overlay analysis; this temporal mismatch is acknowledged here and revisited in Sections 4.3 and 4.4.

Because the overall condition of an aquifer cannot be conveyed by any single determinant, owing to the spatial variability of contaminants and the diversity of measurable indicators; an integrated, GIS-based GQI framework was adopted. The framework synthesises heterogeneous quality data into a single rating that reflects the aggregate condition of the groundwater, and renders the point measurements as a continuous surface suitable for mapping and overlay analysis.

3.2.1. Calculation of the Groundwater Quality Index

The index was computed using the weighted-arithmetic method originally proposed by Horton and developed by Brown *et al.* [9]. The Water Quality Index is defined as the weighted mean of the quality ratings of the individual parameters:

$$\mathrm{WQI} = \sum W_i Q_i \Big/ \sum W_i \tag{1}$$

where n is the number of parameters, W_i is the unit weight of the ith parameter, and Q_i is its quality rating (sub-index). The unit weight is taken to be inversely proportional to the recommended standard for the corresponding parameter:

$$W_i = K/S_n \tag{2}$$

where S_n is the standard permissible value of the ith parameter and K is a proportionality constant. Here K is a proportionality constant determined so that the unit weights sum to unity across the parameter set; it is obtained from:

$$K = 1\Big/\sum\left(1/S_n\right) \tag{3}$$

Following Brown *et al.* [9], the quality rating Q_i is computed as:

$$Q_i = 100\times\left(V_0 - V_i\right)\Big/\left(S_n - V_i\right) \tag{4}$$

where V_0 is the observed value of the parameter at the sampling site and V_i is its ideal value in pure water. The ideal value is taken as zero for all determinands except pH, for which the ideal value is 7.0 (natural water) and the permissible value 8.5. Accordingly, the quality rating for pH is:

$$Q_{pH} = 100\times\left(V_{pH} - 7.0\right)\Big/\left(8.5 - 7.0\right) \tag{5}$$

A rating of $Q_i = 0$ denotes the complete absence of the contaminant; values in the range $0 < Q_i < 100$ indicate concentrations within the permissible standard; and $Q_i > 100$ indicates exceedance of the standard. The resulting index was classified according to the scheme of Brown *et al.* [9].

The standard permissible value (S_n), the ideal value (V_i) and the resulting normalised unit weight (W_i) adopted for each determinand are reported in **Table 2**. Because the unit weight is inversely proportional to the standard, the index is dominated by the parameters with the most stringent guideline values, where manganese ($W_i = 0.756$) and fluoride ($W_i = 0.202$), while pH, nitrate, chloride and electrical conductivity carry progressively smaller weights. Electrical conductivity, which has no WHO health-based guideline, was assigned the Kenya Bureau of Standards limit of 1500 µS/cm as its standard so that it could be incorporated on a consistent basis. With these values, $K = 1/\Sigma(1/S_n) = 0.302$ and the unit weights sum to unity, making the index fully reproducible.

Table 2. Parameter standards, ideal values and normalised unit weights used in the GQI computation.

Parameter (unit)	Standard, S_n	Ideal value, V_i	Unit weight, W_i
pH	8.5	7.0	0.0356
EC (µS/cm)	1500*	0	0.0002
Chloride (mg/L)	250	0	0.0012
Fluoride (mg/L)	1.5	0	0.2015
Nitrate (mg/L)	50	0	0.0060
Manganese (mg/L)	0.4	0	0.7555
Σ	—	—	**1.0000**

$W_i = K/S_n$ with $K = 1/\Sigma(1/S_n) = 0.302$; $\Sigma W_i = 1.0$. *Electrical-conductivity standard after the Kenya Bureau of Standards (1500 µS/cm); all other standards after WHO (2017). The ideal value V_i is taken as zero for all determinands except pH ($V_i = 7.0$).

Table 3 presents borehole identities, physico-chemical determinands and computed groundwater quality index (GQI).

3.2.2. Spatial Modelling and Surface Interpolation

Spatial analysis was performed in ArcGIS 10.8 using the Spatial Analyst and 3D Analyst extensions. Borehole coordinates and elevations were recorded with a handheld GPS to an accuracy of ±5 m and projected to Arc 1960, UTM Zone 37 South. Continuous surfaces for each determinand, and for the composite GQI, were generated from the point observations using inverse-distance weighting (IDW). IDW estimates the value at an unsampled location as a distance-weighted average of neighbouring measurements, assigning greater influence to nearer points; the method is widely applied in groundwater-quality mapping owing to its transparency and modest data requirements [15] [16]. Interpolated parameter values were reclassified against the WHO (2017) thresholds, and the GQI surface

Table 3. Borehole identities, physico-chemical determinands and computed GQI.

No.	Borehole name	pH	EC (μS/cm)	Cl (mg/L)	F (mg/L)	NO_3 (mg/L)	Mn (mg/L)	GQI
1	Dandora Chief's Camp	8.55	404	7	21.6	0.1	0.01	205
2	Kayole Police Station	8.8	341	6	17	0.1	0.01	163
3	Mukuru Kwa Njenga Pr. School	8.45	630	39	11	5.7	0.01	107
4	Olympic Primary School	8.4	592	15.2	14.9	1.3	0.02	146
5	Riruta Satellite Pr. School	7.83	305	15	5	7.3	0.01	51
6	Silanga Undugu Grounds	8.5	382	7	9.6	0.1	0.01	95
7	Huruma Flats	8.04	448	33	1.24	5.2	0.14	60
8	Kenya Union for the Blind	7.99	603	89	0	0.1	0.05	18
9	Kibiku Police Post, Utawala	7.39	606	67	0.05	0.1	0.38	127
10	Mwiki Primary School	7.4	958	190	0.55	5.8	0.04	19
11	Ruai Primary School	7.9	867	99.2	1.25	0.1	0.36	133
12	Tumaini Primary School	7.21	958	130	1.2	0.1	1.45	492
13	G. Development, Muthaiga	7.4	284	20	4	0.1	0.001	38
14	Githogoro-Runda	9.78	248	0.08	0.86	12.63	0.001	13
15	KICD, Ngara	8.3	352	50	7	9.5	0.01	70
16	Kitisuru	8.61	260	12	12.5	0.1	0.001	118
17	Karen	7.68	474	4.4	2.2	0.1	0.01	25

was produced by computing the index at each station and interpolating the result across the aquifer.

The IDW interpolation was implemented in ArcGIS with a power parameter of 2, a search neighbourhood comprising the twelve nearest boreholes, and an output cell size of 90 m (commensurate with the SRTM terrain grid). Because the surfaces are constrained by only seventeen control points, their accuracy is inherently limited: the interpolated GQI is best read as an indicative regional pattern rather than as a precise point predictor, and the uncertainty is greatest in the sparsely sampled periphery. Leave-one-out cross-validation should accompany the interpolation to quantify prediction error, and this constraint is carried into the interpretation of the maps (Section 4.4).

3.3. Land-Use Overlay and Zonal Analysis

To evaluate the influence of land use on groundwater quality, a land-use/land-cover (LULC) classification of Nairobi for 2020 was used. The classified land-use polygons were overlaid on the interpolated GQI surface within the GIS, and zonal statistics were computed to summarise the index within each land-use category. For every class, the mean and standard deviation of the GQI were extracted, enabling a direct, spatially explicit comparison of groundwater quality among built-up, open-space, forest and agricultural land. The standard deviation was retained alongside the mean because it expresses the internal heterogeneity of each land-use class, an important consideration where a single category, such as built-up land, encompasses a wide range of contaminant sources.

Of the eight land-cover classes distinguished in the 2020 map, zonal GQI statistics were computed for four consolidated, hydrologically contrasting analysis classes. To ensure a reproducible mapping, the eight mapped classes were aggregated as follows: built-up combines the built-up and transportation classes (both impervious, urban surfaces); open space combines the open-space, rangeland and riparian/shrub classes (undeveloped or transitional vegetated cover); forest and agriculture are retained as mapped; and water bodies (1% of the area) were excluded as a non-recharge surface without resident boreholes. The four classes therefore account for all recharge-relevant land in the overlay, and this aggregation rule is applied consistently throughout.

Because groundwater quality was summarised as zonal statistics of an interpolated surface rather than as independent measurements within each class, and because the number of boreholes per land-use class is small and unequal, the land-use comparison presented below is descriptive and exploratory rather than inferential. No formal test of between-class differences (for example, a Kruskal–Wallis test) was applied, since its assumptions are not met by seventeen spatially autocorrelated, raster-derived values; the class means should therefore be interpreted as indicative contrasts rather than as statistically confirmed effects. Table 4 presents classification of water quality based on the weighted-arithmetic WQI method.

Table 4. Classification of water quality based on the weighted-arithmetic WQI method.

WQI/GQI range	Rating class
0 - 25	Excellent
26 - 50	Good
51 - 75	Poor
76 - 100	Very poor
>100	Unsuitable

Source: after Brown *et al.* [9].

4. Results and Discussion

4.1. Groundwater Quality

Groundwater quality is fundamental to the sustainability of urban water supply, where populations depend heavily on aquifers for both drinking water and irrigation. The assessment reported here is based on completion-report data for seventeen boreholes distributed across Nairobi County (Table 3), with the descriptive statistics for each determinand summarised in Table 5 and benchmarked against WHO (2017) guidelines.

Spatial Variation of Individual Determinands

pH ranged from 7.21 to 9.78 with a mean of 8.13 and a standard deviation of 0.65, indicating generally alkaline groundwater consistent with other urban aquifers. Most boreholes fall within the WHO acceptable range of 6.5 - 8.5, although Githogoro-Runda recorded an elevated value of 9.78. Such alkalinity is commonly attributable to the dissolution of carbonate minerals but may be reinforced by wastewater discharge and the decay of organic matter; because pH governs the solubility and mobility of metals and nutrients, it functions as a master variable for the overall chemistry of the system. The spatial pattern (**Figure 2**) shows

Table 5. Descriptive statistics of the parameters used to compute the GQI, with WHO (2017) guideline values.

No.	Parameter (units)	WHO (2017)	Min.	Max.	Mean	Std. dev.
1	pH	7–8	7.21	9.78	8.13	0.65
2	EC (μS/cm)	—	248	958	512.47	234.29
3	Chloride (mg/L)	250	0.08	190	46.11	53.25
4	Fluoride (mg/L)	1.5	0	21.6	6.47	6.78
5	Nitrate (mg/L)	50	0.1	12.63	2.85	4.03
6	Manganese (mg/L)	0.1–0.4	0.001	1.45	0.15	0.36

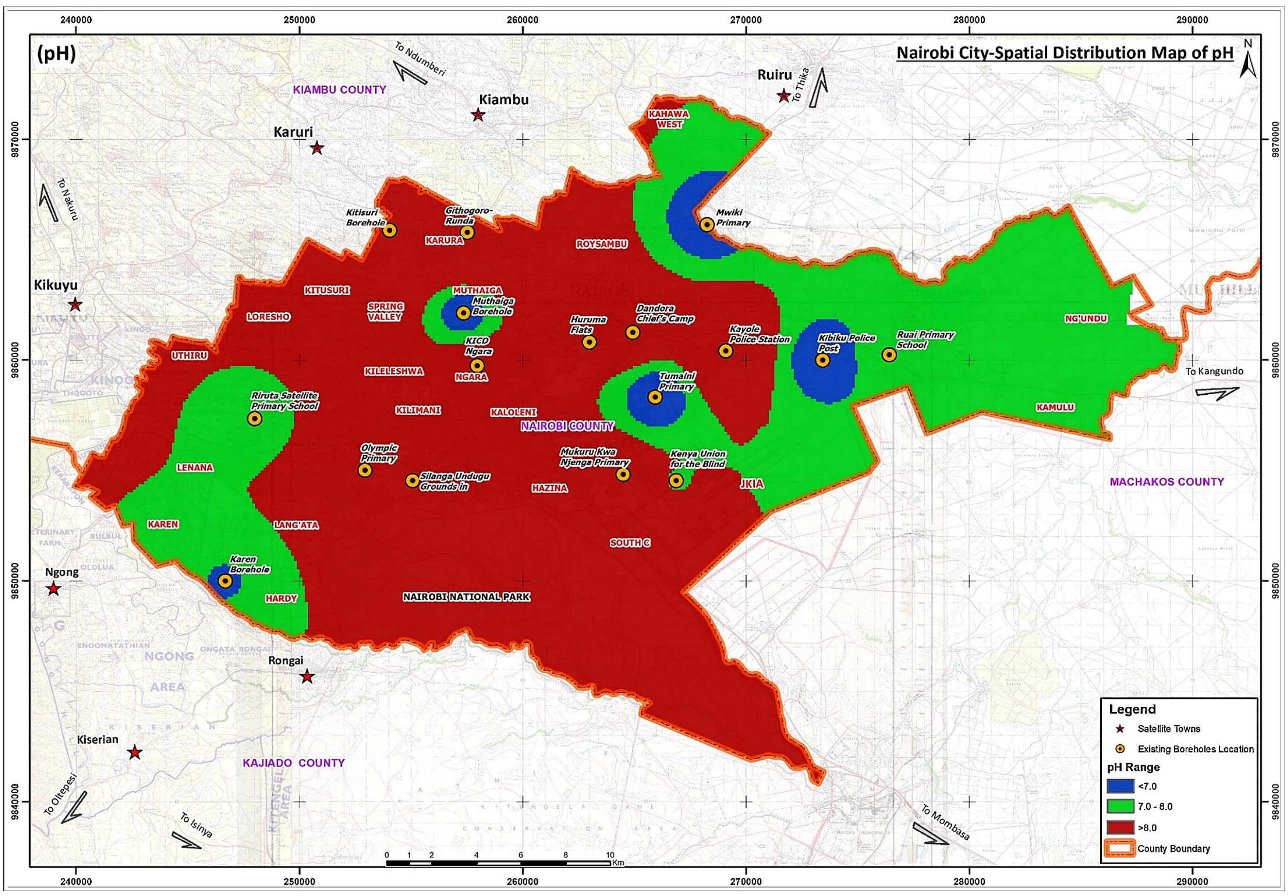

Figure 2. Spatial distribution of pH across the study area.

elevated values concentrated in the central and southern parts of the aquifer.

Electrical conductivity ranged from 248 to 958 µS/cm (mean 512.47 µS/cm), remaining well below the 1500 µS/cm guideline of the Kenya Bureau of Standards and indicating that the groundwater is not appreciably saline. The variability among boreholes nevertheless reveals spatial differences in dissolved-solids content, with the highest values at Mwiki and Tumaini primary schools (**Figure 3**). These maxima coincide with densely settled districts, suggesting a contribution from urban runoff and localised contamination; the comparatively low conductivities elsewhere are consistent with the volcanic lithology and the distance from saline sources [17] [18].

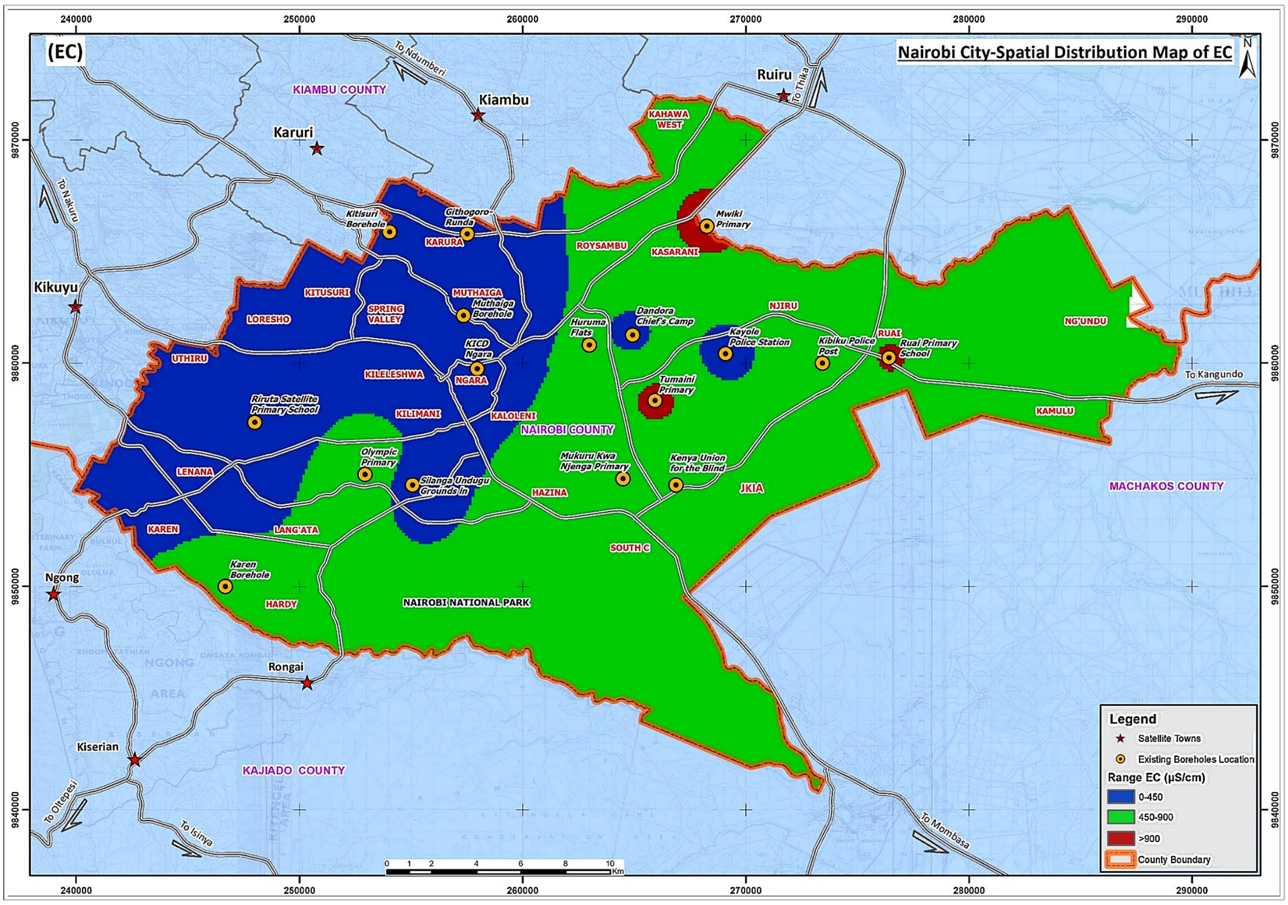

Figure 3. Spatial distribution of electrical conductivity across the study area.

Nitrate concentrations ranged from 0.1 to 12.63 mg/L (mean 2.85 mg/L), comfortably below the WHO limit of 50 mg/L, indicating broad compliance for this determinand. The highest value, 12.63 mg/L at Githogoro-Runda, together with elevated levels near Mukuru Kwa Njenga, points to localised, point-source loading from on-site sanitation and nearby cultivation (**Figure 4**). As nitrate is a sensitive and conservative tracer of anthropogenic influence, its distribution provides an early indication of the pressures that a sustained increase in waste and fertiliser loading could exert on the aquifer [19] [20].

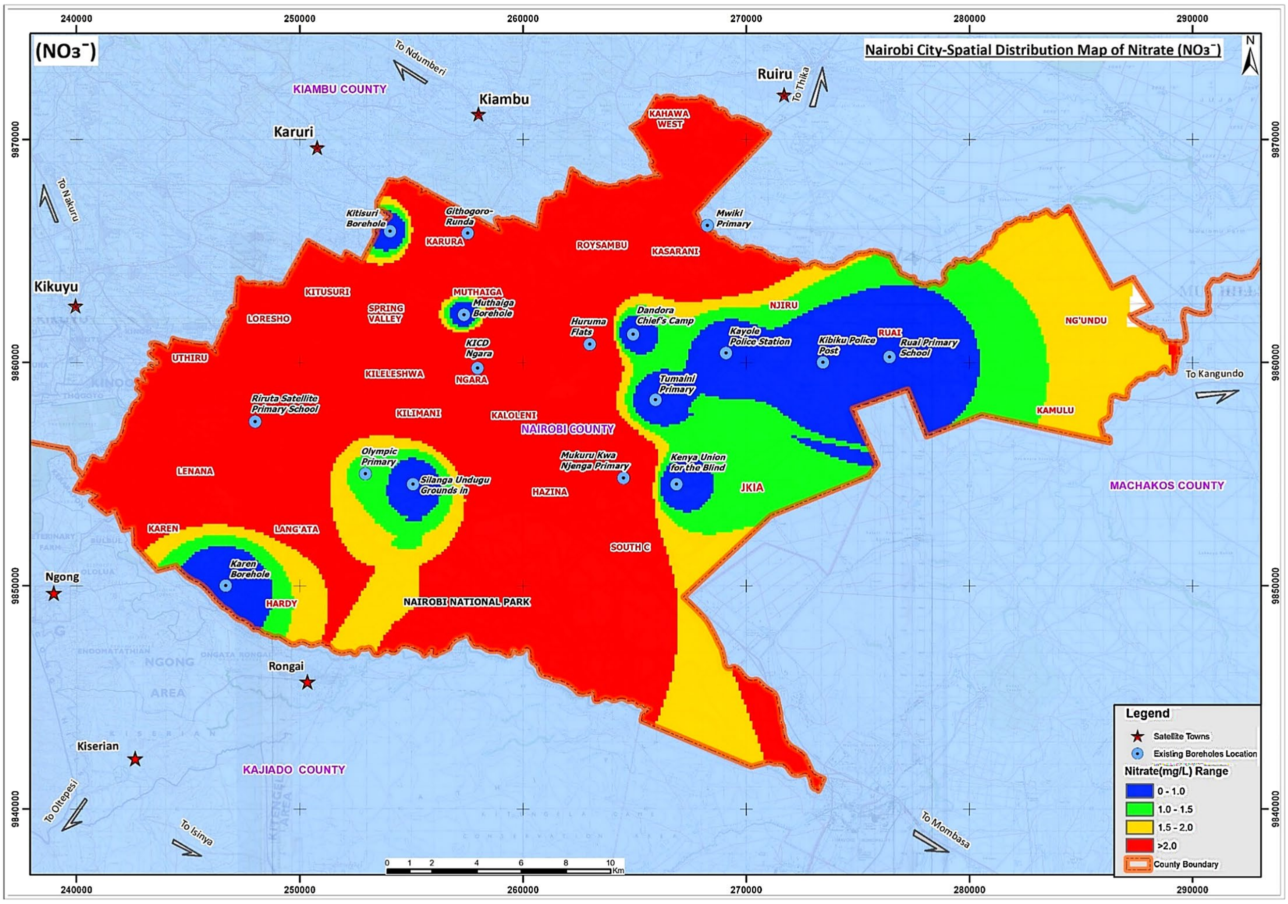

Figure 4. Spatial distribution of nitrate across the study area.

Chloride ranged widely from 0.08 to 190 mg/L (mean 46.11 mg/L), with the maximum recorded at Mwiki Primary School and the minimum at Githogoro-Runda (Figure 5). Although the great majority of boreholes lie below the WHO guideline of 250 mg/L, the elevated values at Mwiki and at the Kenya Union for the Blind indicate localised susceptibility to contamination from wastewater discharge and other urban activities. Because chloride is mobile and persistent, it is a useful indicator of pollution pathways and of the influence of the surrounding land use.

Fluoride ranged from 0 to 21.6 mg/L (mean 6.47 mg/L), with the highest concentrations at Dandora Chief's Camp (21.6 mg/L) and Olympic Primary School (14.9 mg/L), and the lowest at the Kenya Union for the Blind and Githogoro-Runda (Figure 6). The mean substantially exceeds the WHO guideline of 1.5 mg/L, and the exceedances are most plausibly geogenic in origin: the spatial pattern tracks the fluoride-rich trachytic and phonolitic volcanics characteristic of the Kenyan Rift, whose weathering releases fluoride to groundwater largely independently of surface land use. Anthropogenic pathways such as waste disposal and phosphate-fertiliser use may locally augment these concentrations, but the regional signal is dominated by lithology, and the two contributions cannot be fully separated with the present data. Prolonged exposure at these levels is

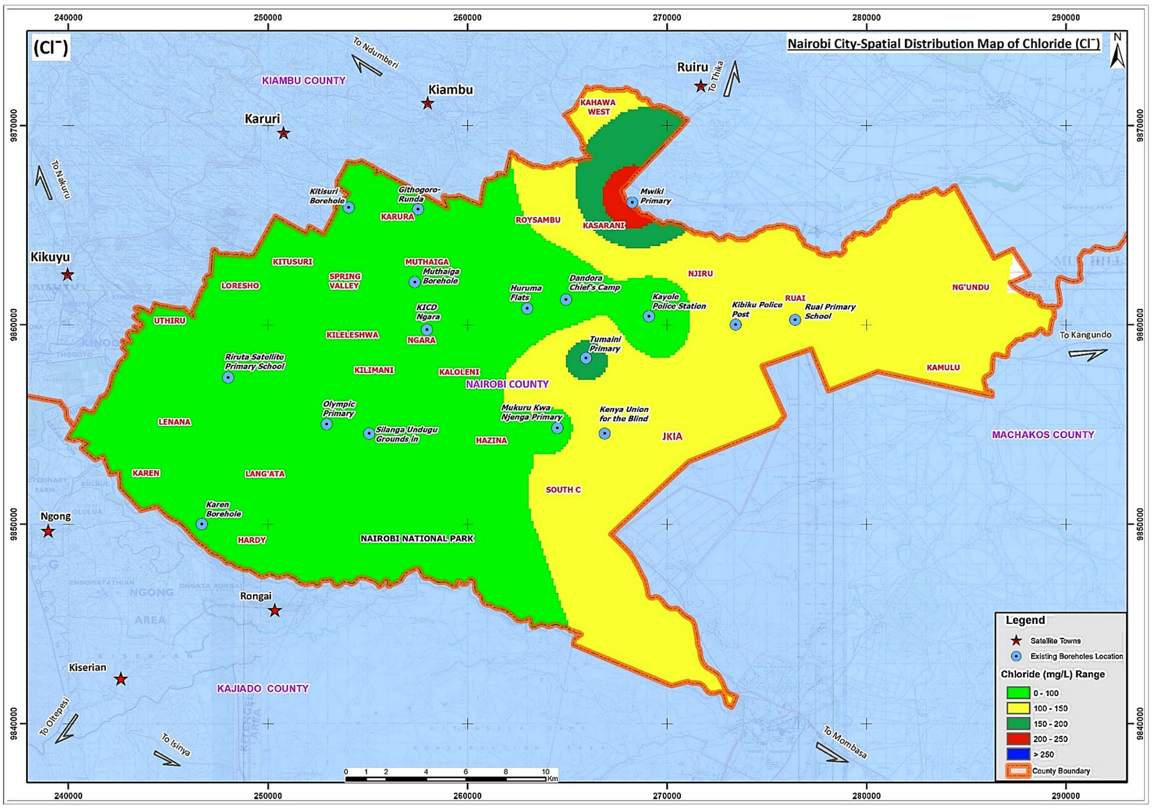

Figure 5. Spatial distribution of chloride across the study area.

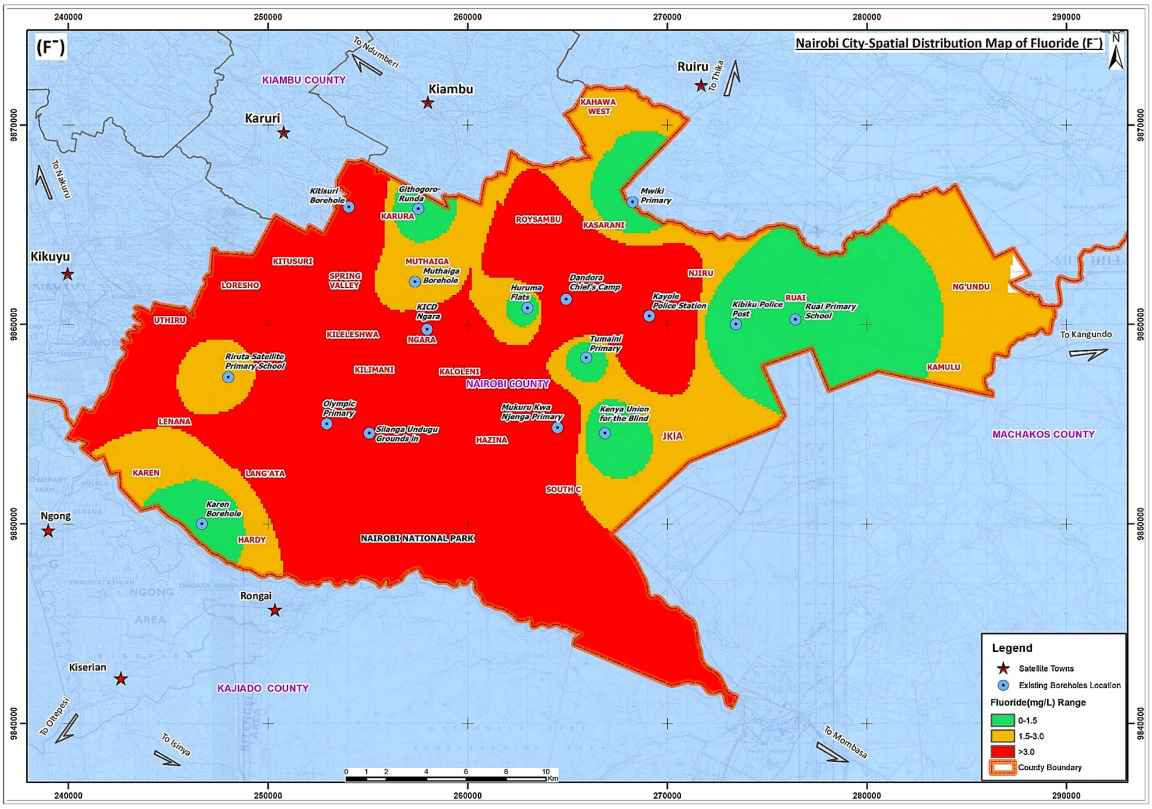

Figure 6. Spatial distribution of fluoride across the study area.

associated with dental and skeletal fluorosis, making fluoride one of the most health-relevant determinands in the study area and a priority for targeted monitoring.

Manganese ranged from 0.001 to 1.45 mg/L (mean 0.15 mg/L), with elevated values at Huruma Flats and a marked maximum of 1.45 mg/L at Tumaini Primary School (**Figure 7**). Several boreholes exceed the WHO guideline of 0.4 mg/L. While trace manganese is an essential nutrient, higher concentrations impart undesirable taste and staining and, in excess, are associated with neurological effects, particularly in children. The distribution is likewise best explained primarily by geogenic processes, reductive dissolution of manganese from the volcanic substrate under the locally circumneutral-to-alkaline, low-oxygen conditions of the aquifer, rather than by land use alone. The isolated maximum at Tumaini Primary School, however, coincides with a densely built-up setting and may reflect an additional, redox-altering anthropogenic input; distinguishing the geogenic baseline from such local enhancements will require targeted, depth-resolved sampling.

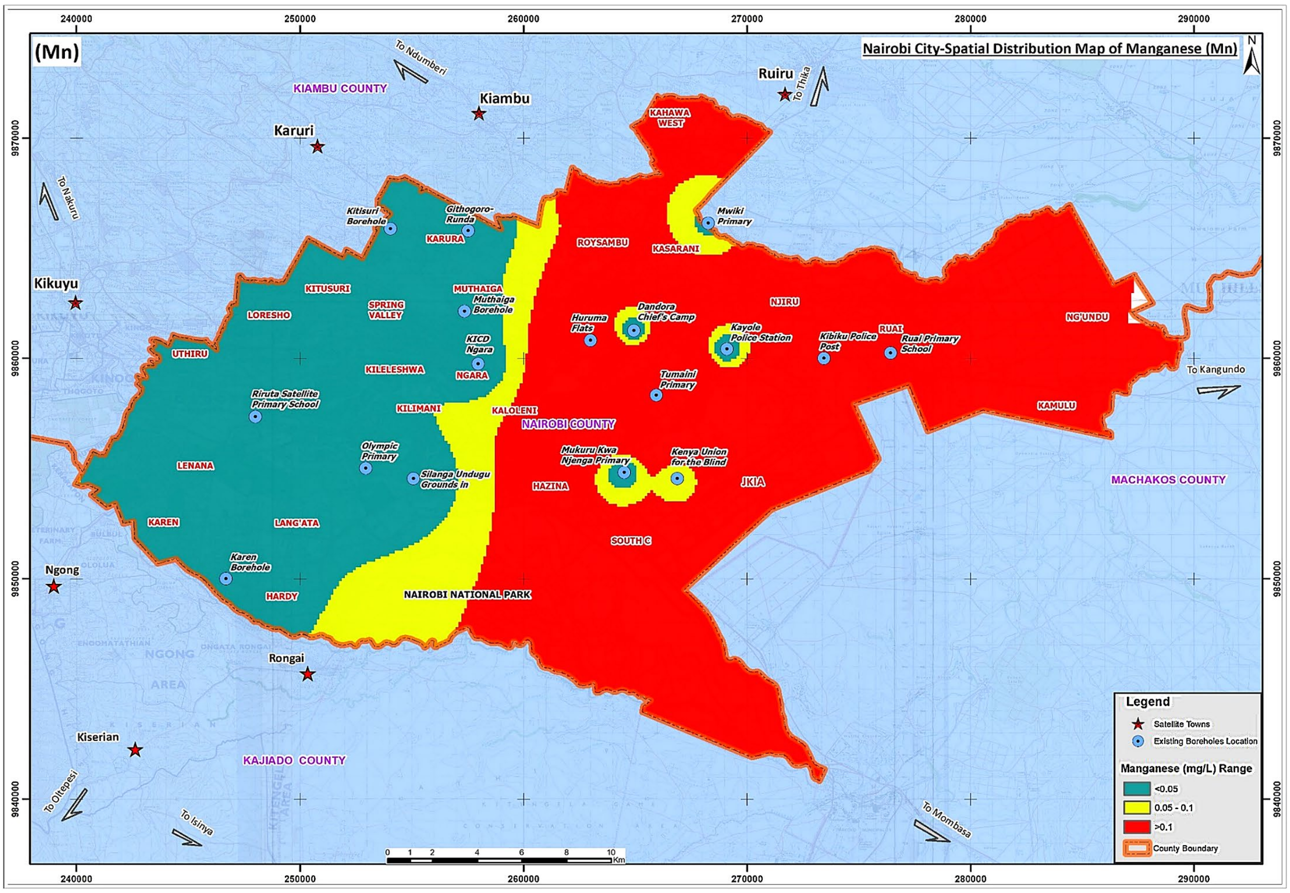

Figure 7. Spatial distribution of manganese across the study area.

4.2. Results for GQI

The composite GQI ranged from 13 to 492, confirming pronounced spatial heterogeneity in groundwater quality across the aquifer (**Table 3**; **Figure 8**). Under the classification of **Table 4**, Githogoro-Runda (13) and the Kenya Union for the

Blind (18) returned "excellent" water, whereas Tumaini Primary School (492) represents the most degraded site. Elevated indices cluster in the densely populated central and eastern districts: Dandora Chief's Camp (205), Kayole Police Station (163), Ruai (133), Kibiku (127) and Mukuru Kwa Njenga (107), where proximity to on-site sanitation, solid-waste leachate and surface runoff increases contaminant loading. Conversely, the lowest indices coincide with the vegetated, less-developed western and peri-urban margins.

The spatial coherence of the index is informative: high-GQI cores correspond to the same districts that recorded peak chloride, manganese and conductivity, indicating that the composite measure successfully integrates the individual signals into a single, interpretable surface. The strong gradient from the urban core to the vegetated periphery foreshadows the land-use dependence examined in Section 4.3.

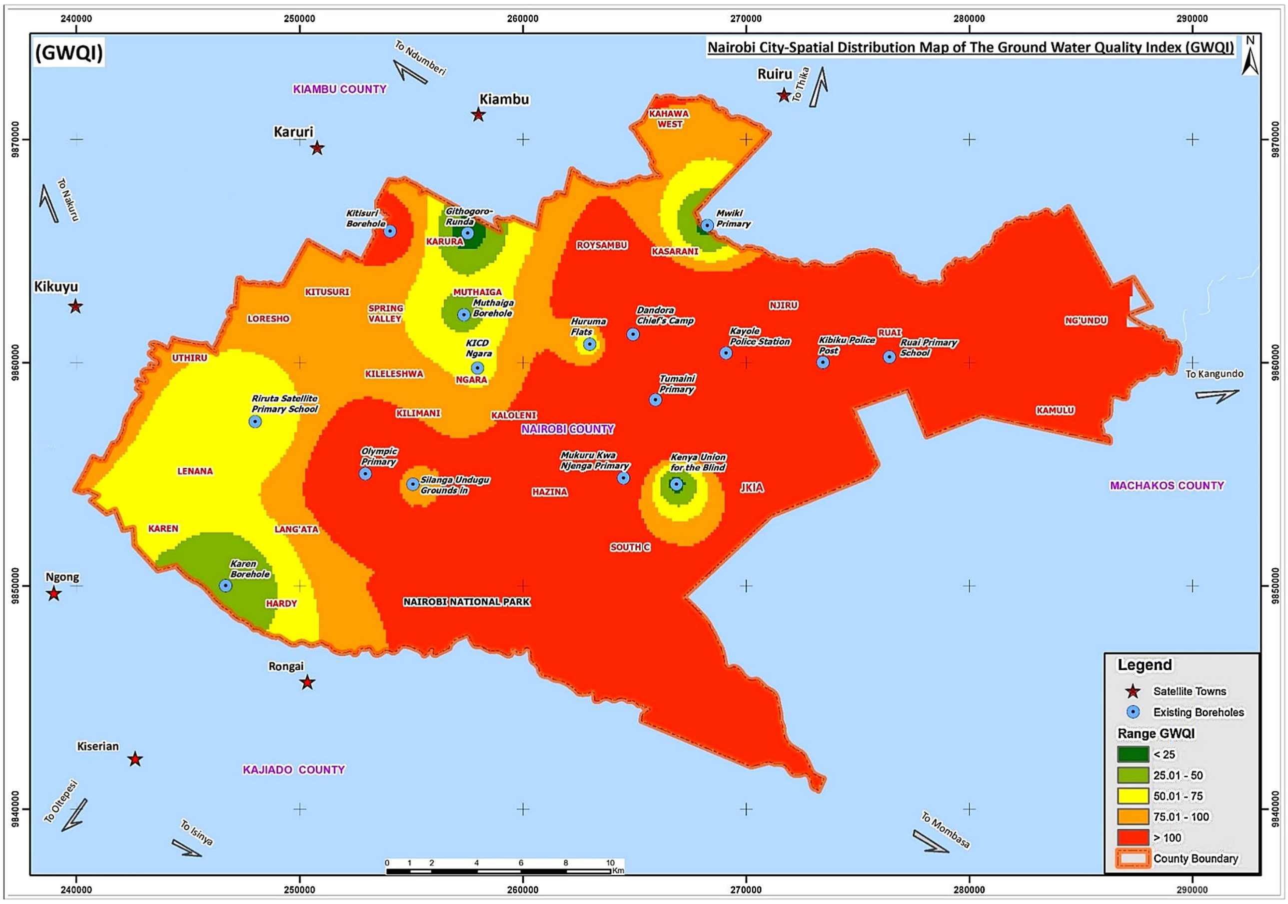

Figure 8. Spatial distribution of the Groundwater Quality Index (GQI) of the Nairobi Aquifer.

4.3. Influence of Land Use on Groundwater Quality

Land use exerts a clear and systematic influence on groundwater quality in the study area. The land-use classification (**Figure 9**) shows that built-up land dominates the central aquifer, with agriculture, open space, forest and riparian cover distributed across the periphery; the corresponding area shares are summarised in **Figure 10**, in which built-up land accounts for 32% of the mapped area, rangeland

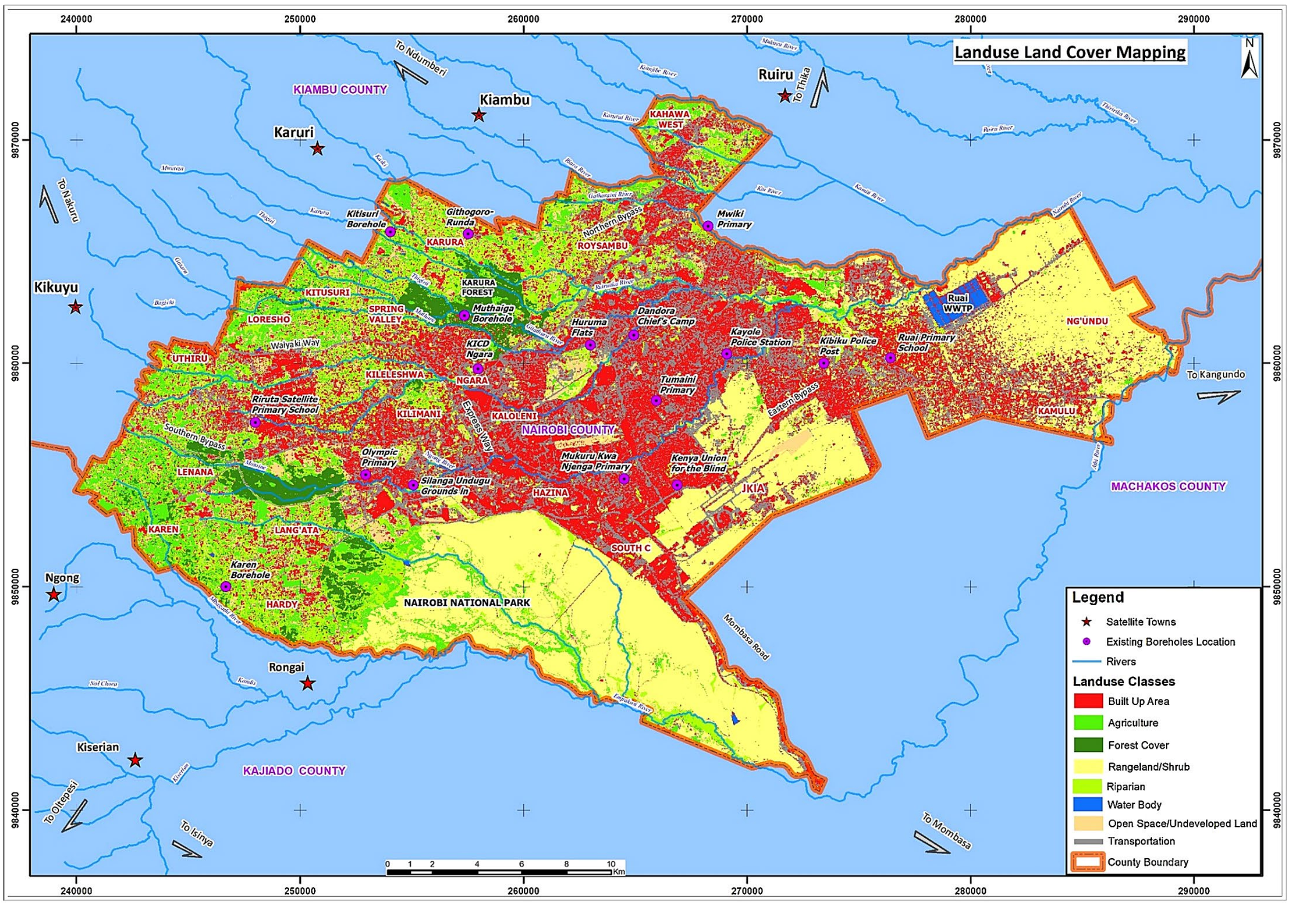

Figure 9. Land-use/land-cover classification of the Nairobi Aquifer.

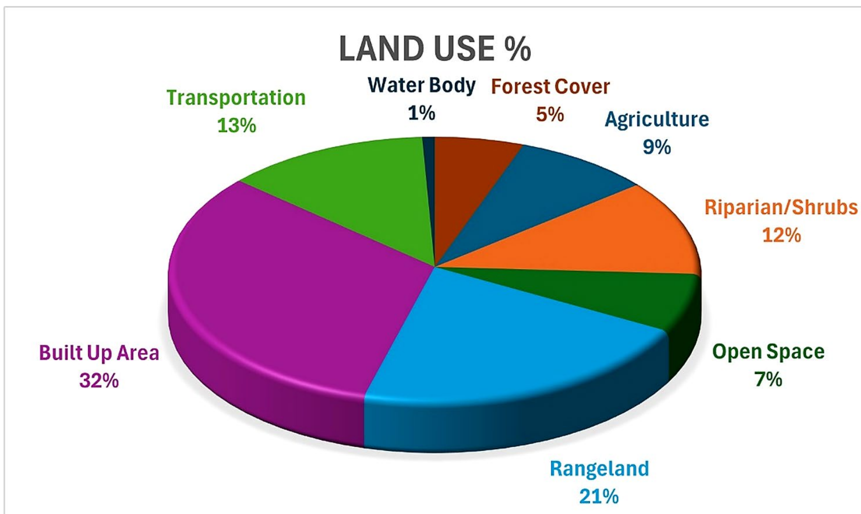

Figure 10. Percentage area of each land-use type in the study area.

21%, transportation 13%, riparian/shrub 12%, agriculture 9%, open space 7%, forest 5% and water bodies 1%.

Overlaying the land-use polygons on the GQI surface and computing zonal statistics produced the class-wise summary in **Table 6**. Built-up land exhibited the highest mean GQI (150.2), placing it in the "unsuitable" category, while forest cover returned the lowest mean (38, "good"). Open space and agriculture occupied intermediate positions, with means of 61.3 and 52, respectively. The monotonic ordering: forest < agriculture < open space < built-up—is consistent with the degree of anthropogenic modification of the land surface being an important control on groundwater quality, with impervious, intensively used urban land driving the greatest degradation and natural vegetation conferring a protective effect.

The within-class variability is equally informative. Built-up land displayed by far the largest standard deviation (132.6), reflecting the heterogeneity of urban contaminant sources, ranging from leaking sewers and pit latrines to fuel handling and informal solid-waste disposal, whose intensity varies sharply over short distances. Agriculture also showed appreciable spread (57.5), consistent with the patchy application of fertilisers and agrochemicals, whereas forest cover showed essentially none (0.0), underscoring the consistency of good-quality groundwater beneath undisturbed vegetation. This dispersion has direct management implications: in built-up zones, the high mean and high variance together imply that aquifer protection cannot rely on area-wide measures alone but must target specific, locally dominant sources.

These findings are consistent with the broader literature linking urbanisation and intensive cultivation to groundwater-quality decline. Impervious surfaces increase runoff and the rapid transfer of surface-derived contaminants to the subsurface, while fertilisers and pesticides associated with cultivation leach toward the water table; both mechanisms are amplified in the low-relief, densely settled core of Nairobi, where the highest-GQI boreholes coincide with the largest built-up footprint [12] [13] [21]. The convergence of the index pattern (**Figure 8**) and the land-use pattern (**Figure 9**) provides spatially explicit evidence that land-use type is an important correlate of groundwater quality in the aquifer, within the descriptive limits noted above.

Table 6. Groundwater Quality Index statistics for each land-use type.

No.	Land-use type	Mean GQI	Std. dev.	Rating class
1	Built-up areas	**150.2**	132.6	Unsuitable
2	Open space/undeveloped land	**61.3**	38.7	Poor
3	Forest cover	**38**	0.0	Good
4	Agriculture	**52**	57.5	Poor

4.4. Limitations

Several limitations qualify the interpretation of these results and define priorities for future work. First, the study relies almost entirely on secondary data: the water-chemistry records were extracted from WRA borehole completion reports rather than from a purpose-designed sampling campaign, and the terrain, soil, rainfall and land-cover layers were drawn from existing national and international repositories, some dating to 2020. This constrains both the choice of determinands and the currency of the information. The six available parameters (pH, EC, chloride, fluoride, nitrate and manganese) omit constituents central to a full potability and health assessment, temperature, turbidity, microbiological indicators such as Escherichia coli, and dissolved heavy metals, so the GQI reported here characterises the salinity-nutrient-trace-metal dimension of quality rather than microbiological safety.

Second, the borehole network is small (n = 17) and was assembled purposively on the basis of data completeness and spatial spread rather than through a formal, power-based sampling design; no sample-size calculation underlies the selection, and completion dates, depths and screened intervals are only partially documented, limiting assessment of whether the sites sample comparable horizons of the multi-layered aquifer. Third, the chemical records are largely undated relative to a single common survey and were not corrected for seasonal variation; because recharge and contaminant transport in this aquifer are strongly seasonal, values collected under different conditions may not be directly comparable, and paired dry- and wet-season sampling would strengthen future assessments. Fourth, the completion-report chemistry is not fully contemporaneous with the 2020 land-cover map, introducing a temporal mismatch into the overlay. Fifth, with only seventeen control points the interpolated GQI surface carries substantial uncertainty, and the land-use comparison is accordingly treated as descriptive rather than inferential. Finally, some of the interpolated maps (**Figures 2-9**) would benefit from higher-resolution rendering and enlarged legends to improve legibility. Addressing these limitations, through denser, purpose-designed and seasonally paired sampling, a broader determinand suite, fuller borehole metadata, and formal cross-validation of the interpolated surfaces, would place the land-use–quality relationship identified here on a firmer inferential footing.

5. Conclusions

This study determined the groundwater quality index of the Nairobi Aquifer using GIS techniques and evaluated the influence of land-use type on that quality. Drawing on six physico-chemical determinands for seventeen boreholes, a weighted-arithmetic GQI was computed, interpolated by inverse-distance weighting and overlaid on a contemporary land-use classification through zonal analysis.

The GQI ranged from 13 to 492, revealing strong spatial heterogeneity, with the most degraded groundwater concentrated in the densely settled central and eastern districts and the best quality on the vegetated periphery. Among individual determinands, fluoride and manganese most frequently exceeded WHO guidelines, while nitrate, chloride and conductivity remained largely compliant but displayed localised maxima diagnostic of anthropogenic loading.

Land-use type emerged as an important correlate of groundwater quality. Mean GQI increased monotonically from forest cover (38, "good") through agriculture

(52) and open space (61.3) to built-up land (150.2, "unsuitable"), and the exceptionally large within-class variance of built-up land (132.6) reflects the diversity and spatial concentration of urban contaminant sources. Together, these results identify urbanization, and its associated impervious surfaces, on-site sanitation and waste streams—as the land-use category most strongly associated with groundwater degradation, with natural vegetation coinciding with the best-quality groundwater.

The maps and statistics presented here constitute a decision-ready evidence base for prioritising groundwater protection in Nairobi. They argue for the explicit integration of aquifer safeguards into urban land-use planning, for source-specific interventions in high-GQI built-up zones, and for the establishment of a sustained monitoring network. Future work should extend the determinand suite to microbiological and emerging contaminants, increase borehole density to refine the interpolated surfaces, and couple the GQI with intrinsic-vulnerability modelling to support a fully risk-based management framework.

Conflicts of Interest

The authors declare no conflicts of interest regarding the publication of this paper.

References

[1] Foster, S., Chilton, J., Nijsten, G. and Richts, A. (2013) Groundwater—A Global Focus on the 'Local Resource'. *Current Opinion in Environmental Sustainability*, **5**, 685-695. https://doi.org/10.1016/j.cosust.2013.10.010

[2] Calow, R.C., MacDonald, A.M., Nicol, A.L. and Robins, N.S. (2010) Ground Water Security and Drought in Africa: Linking Availability, Access, and Demand. *Groundwater*, **48**, 246-256. https://doi.org/10.1111/j.1745-6584.2009.00558.x

[3] Kumar, C.P. (2018) Water Security—Challenges and Needs. *International Journal of Engineering Sciences & Research Technology*, **7**, 26-29.

[4] Adelana, S. and MacDonald, A. (2008) Applied Groundwater Studies in Africa. IAH Selected Papers on Hydrogeology, Volume 13. CRC Press. https://doi.org/10.1201/9780203889497

[5] Giordano, M. (2009) Global Groundwater? Issues and Solutions. *Annual Review of Environment and Resources*, **34**, 153-178. https://doi.org/10.1146/annurev.environ.030308.100251

[6] Mumma, A., Lane, M., Kairu, E., Tuinhof, A. and Hirji, R. (2011) Kenya Ground-Water Governance Case Study. Water Papers, World Bank.

[7] Yin, L., Hou, G., Su, X., Wang, D., Dong, J., Hao, Y., et al. (2013) Isotopes (δD and δ^{18}O) in Precipitation, Groundwater and Surface Water in the Ordos Plateau, China. *Hydrogeology Journal*, **19**, 429-443.

[8] Dams, J., Woldeamlak, S.T. and Batelaan, O. (2008) Predicting Land-Use Change and Its Impact on the Groundwater System of the Kleine Nete Catchment, Belgium. *Hydrology and Earth System Sciences*, **12**, 1369-1385. https://doi.org/10.5194/hess-12-1369-2008

[9] Brown, R.M., McClelland, N.I., Deininger, R.A. and O'Connor, M.F. (1972) A Water Quality Index—Crashing the Psychological Barrier. In: Thomas, W.A., Ed., *Indicators of Environmental Quality*, Springer, 173-182.

https://doi.org/10.1007/978-1-4684-2856-8_15

[10] Ram, A., Tiwari, S.K., Pandey, H.K., Chaurasia, A.K., Singh, S. and Singh, Y.V. (2021) Groundwater Quality Assessment Using Water Quality Index (WQI) under GIS Framework. *Applied Water Science*, **11**, Article No. 46. https://doi.org/10.1007/s13201-021-01376-7

[11] Karuppannan, S. and Serre Kawo, N. (2020) Groundwater Quality Assessment Using Geospatial Techniques and WQI in North East of Adama Town, Oromia Region, Ethiopia. *Hydrospatial Analysis*, **3**, 22-36. https://doi.org/10.21523/gcj3.19030103

[12] Scanlon, B.R., Reedy, R.C., Stonestrom, D.A., Prudic, D.E. and Dennehy, K.F. (2005) Impact of Land Use and Land Cover Change on Groundwater Recharge and Quality in the Southwestern Us. *Global Change Biology*, **11**, 1577-1593. https://doi.org/10.1111/j.1365-2486.2005.01026.x

[13] Khan, A., Khan, H.H. and Umar, R. (2017) Impact of Land-Use on Groundwater Quality: Gis-Based Study from an Alluvial Aquifer in the Western Ganges Basin. *Applied Water Science*, **7**, 4593-4603. https://doi.org/10.1007/s13201-017-0612-7

[14] Rendilicha, H.G., Home, P., Raude, J.M., M'Erimba, C.M. and Muthoka, S. (2020) Assessing the Impact of Land-Use Types on the Groundwater Quality: A Case Study of Mid River Njoro Catchment, Kenya. *Acque Sotterranee—Italian Journal of Groundwater*, **9**, 39-47. https://doi.org/10.7343/as-2020-350

[15] Tomczak, M. (1998) Spatial Interpolation and Its Uncertainty Using Automated Anisotropic Inverse Distance Weighting (IDW)-Cross-Validation/Jackknife Approach. *Journal of Geographic Information and Decision Analysis*, **2**, 18-30.

[16] Mueller, T.G., Pusuluri, N.B., Mathias, K.K., Cornelius, P.L., Barnhisel, R.I. and Shearer, S.A. (2004) Map Quality for Ordinary Kriging and Inverse Distance Weighted Interpolation. *Soil Science Society of America Journal*, **68**, 2042-2047. https://doi.org/10.2136/sssaj2004.2042

[17] McCall, G.J.H. (1967) Geology of the Nakuru-Thomson's Falls-Lake Hannington Area. Geological Survey of Kenya, Report No. 78.

[18] Baker, B.H. (1986) Tectonics and Volcanism of the Southern Kenya Rift Valley and Its Influence on Rift Sedimentation. *Geological Society*, *London*, *Special Publications*, **25**, 45-57. https://doi.org/10.1144/gsl.sp.1986.025.01.05

[19] Fuhrer, G.J., Gilliom, R.J., Hamilton, P.A., Morace, J.L., Nowell, L.H., Rinella, J.F. and Wentz, D.A. (1999) The Quality of Our Nation's Waters: Nutrients and Pesticides. US Geological Survey Circular 1225.

[20] Baalousha, H.M. (2011) Mapping Groundwater Contamination Risk Using GIS and Groundwater Modelling. A Case Study from the Gaza Strip, Palestine. *Arabian Journal of Geosciences*, **4**, 483-494. https://doi.org/10.1007/s12517-010-0135-0

[21] Mishra, N., Khare, D., Gupta, K.K. and Shukla, R. (2014) Impact of Land Use Change on Groundwater: A Review. *Advances in Water Resource and Protection*, **2**, 28-41.